Talanta 116 (2013) 991–996

Contents lists available at ScienceDirect

Talanta

journal homepage: www.elsevier.com/locate/talanta

Amperometric phenol biosensor based on covalent immobilization of tyrosinase on Au nanoparticle modified screen printed carbon electrodes

Md. Nurul Karim, Hye Jin Lee*

Department of Chemistry and Green-Nano Materials Research Center, Kyungpook National University, 1370 Sankyuk-dong, Buk-gu, Daegu 702-701, Republic of Korea

ARTICLE INFO

Article history:
Received 19 June 2013
Received in revised form
6 August 2013
Accepted 6 August 2013
Available online 16 August 2013

Keywords:
Amperometric biosensor
Phenol
Tyrosinase
Gold nanoparticle
Screen printed carbon electrode

ABSTRACT

A highly selective and sensitive amperometric biosensor for the detection of phenol was developed based on a platform where Au nanoparticles (AuNPs) are electrodeposited onto a disposable screen printed carbon electrode and tyrosinase is then covalently immobilized on the AuNP's using alkanethiol and cross-linker molecules. The electrocatalytic responses of the tyrosinase modified biosensor for the detection of phenol were measured using both cyclic voltammetry and square wave voltammetry. Temperature, buffer pH and the amount of tyrosinase immobilized on the electrode surface were also optimized for phenol sensing. A high sensitivity of 15.7 μA ppm^{-1}, a low detectable phenol concentration of 47 ppb alongside a linear response from 47 ppb to 15 ppm was achieved using square wave voltammetry in addition to good selectivity. As a demonstration, the biosensor was applied to determine phenol concentrations in regional water samples from S. Korea.

1. Introduction

Phenol is a toxic pollutant which is a serious potential hazard for human health and aquatic life. It is often released into aquatic environments due to its wide industrial application. Owing to its toxicity, the US Environmental Protection Agency (EPA) and the European Union (EU) have now listed phenol as a priority toxic pollutant and set a standard permeable total limit of 0.5 ppb in drinking water [1]. A wide spectrum of analytical techniques including gas chromatography/mass spectrometry, liquid chromatography, capillary electrophoresis and ultraviolet spectrophotometry [2–5] are now conventionally used for monitoring phenol. However, these methods are more often require complicated sample pretreatment and inconvenient for field or on-site monitoring applications. Alternatively, amperometric biosensors can offer an excellent alternative due to their diverse advantages including compact nature, rapid response, low cost, low power consumption and easy handling in field applications [6].

There have been extensive research works for the amperometric detection of phenol in particular utilizing the enzyme, tyrosinase [7–9], since it is known to selectively catalyze the oxidation of phenol via catechol to *o*-quinone in the presence of molecular oxygen [8–10]. The key aspect in the construction of such an enzyme modified amperometric biosensor is to efficiently immobilize enzyme molecules onto the sensor surface. In recent years, a wide range of surface linking methods for tethering enzymes onto various types of electrochemical sensor surfaces have been developed including physical adsorption [11], sol–gels [12], the electrochemical entrapment of enzymes within a polymer or a composite matrix [13,14], incorporation within carbon paste [15] and covalent cross-linking [16–18].

In addition to the robust attachment of enzymes onto sensor surfaces, improvements in the sensitivity of biosensors are an important issue, which can help the sensors be applied to the analysis of trace level of target contaminants in environmental samples. Detection sensitivity has been greatly advanced by the use of nanomaterials in conjunction with enzyme modified electrochemical sensors [19,20]. In particular, gold nanoparticles (AuNPs) have been used because of their excellent electrical properties, large active surface areas for enzyme immobilization, capabilities for reducing bioreceptor-metal particles distances in addition to good catalytic activities and biocompatibility [21]. Also, AuNPs can enable the robust immobilization of enzymes via the combined use of alkanethiol self-assembly and cross-linking chemistry [22]. Incorporation of NPs onto sensor electrode surfaces can usually be achieved via direct citrate reduction [23], seeded growth synthesis [24], laser ablation method [25], sol–gels [26], electrodeposition [27] and attachment by a polymer film [28].

* Corresponding author. Tel.: +82 053 950 5336.
E-mail address: hyejinlee@knu.ac.kr (H.J. Lee).

0039-9140/$ - see front matter © 2013 Elsevier B.V. All rights reserved.
http://dx.doi.org/10.1016/j.talanta.2013.08.003

Among these, controlled electrodeposition offers an easy and rapid way for the creation of gold nanoparticles on the electrode surface for biosensing applications [29].

In this paper, we demonstrate a portable in-situ amperometric biosensor composed of surface-immobilized gold nanoparticles (AuNPs) and tyrosinase on screen printed carbon electrodes (SPE) for the selective and sensitive detection of phenol. The combined use of each of these design components is important to create a robust and sensitive platform capable of repeat measurements in a field setting. AuNPs were first electrodeposited on a custom made screen printed electrode. Tyrosinase was then covalently attached to the carboxylic acid terminated AuNP surface using *N*-(3-dimethylaminopropyl)-*N′*-ethylcarbodiimide hydrochloride and *N*-hydroxysulfosuccinimide (EDC/NHSS). Cyclic (CV) and square wave (SWV) voltammetries were employed for the selective and sensitive sensing of phenol. As a demonstration, the biosensor was applied to analyze phenol contamination in some regional water samples from the Sincheon river in Daegu city (S. Korea) and the result was verified with that of autoanalyzer from the *Korea Environment & Water Works Institute*, one of the Korean-certified water quality evaluation centers.

2. Experimental

2.1. Reagents and solutions

Tyrosinase (4964 U mg^{-1} from mushroom, Sigma-Aldrich), gold (III) chloride trihydrate ($HAuCl_4$, Sigma-Aldrich), 3-mercaptopropionic acid (MPA, Sigma-Aldrich), *N*-(3-dimethylaminopropyl)-*N′*-ethylcarbodiimide hydrochloride (EDC, Thermo), *N*-hydroxysulfosuccinimide (NHSS, Thermo), dipotassium hydrogen phosphate (K_2HPO_4, Merck), potassium dihydrogenphosphate (KH_2PO_4, Merck), phenol (DC Chemical Co. Ltd.), sulfuric acid, 95%, (OCI Company Ltd.) and ethanol (Merck) were all used as received. A 0.1 M phosphate buffer solution at pH 7.0 was used for phenol analysis unless otherwise specified, and the stock solution of phenol prepared in the phosphate buffer solution was freshly made for each set of experiments. All aqueous solutions were prepared using Millipore-filtered water.

2.2. Apparatus and electrodes

Electrodeposition and all electrochemical measurements including chronoamperometry, CV and SWV were performed using a computer controlled potentiostat (Autolab PGSTAT128N Ecochemie, Netherland) with General Purpose Electrochemical System (GPES) version 4.9 software package. Scanning electron microscopy (SEM) images were obtained using a HITACHI S-4800 model (KBSI, Daegu, S. Korea). Screen printed electrodes (SPE) were custom made in a local company (The BIO Co., Ltd., S. Korea) consisted of a carbon working electrode (geometric working area: 28 mm^2), a carbon counter electrode, and a Ag/AgCl reference electrode (Fig. S1b). A sensor connector was used to connect SPE's with the potentiostat. A photograph showing our portable phenol sensor is also included in the Supporting Information (Fig. S2).

2.3. Preparation of gold nanoparticle modified SPE

Gold nanoparticles (AuNPs) were electrodeposited onto the working electrode in SPE using a chronoamperometric approach modifying the method from Alonso-Lomillo et al. [22]; a constant potential of 0.18 V (vs. Ag/AgCl) was applied for 400 s to the SPE immersed into a 0.5 mM $HAuCl_4$ in 0.5 M H_2SO_4 solution under stirring condition. The AuNP deposited SPE was then washed three times with water and dried under a N_2 stream prior to use.

2.4. Biosensor preparation

The fabrication of the tyrosinase and AuNP modified SPE is illustrated in Scheme 1. A AuNP coated SPE was then immersed in 40 mM MPA solution (75/25, v/v, absolute ethanol/water) for 15 h at room temperature resulting in the self assembled formation of a carboxylic acid terminated monolayer onto the AuNP surface [22]. The excess MPA was then removed by the subsequent rinsing of the electrode with ethanol and water several times and dried under nitrogen gas. Next, the MPA modified AuNP–SPE sensor was exposed to 50 μL of 75 mM EDC and 15 mM NHSS in 50 mM phosphate buffer solution (pH 7.4) for 30 min. A 16 μL aliquot of tyrosinase (1 mg/mL in 50 mM phosphate buffer

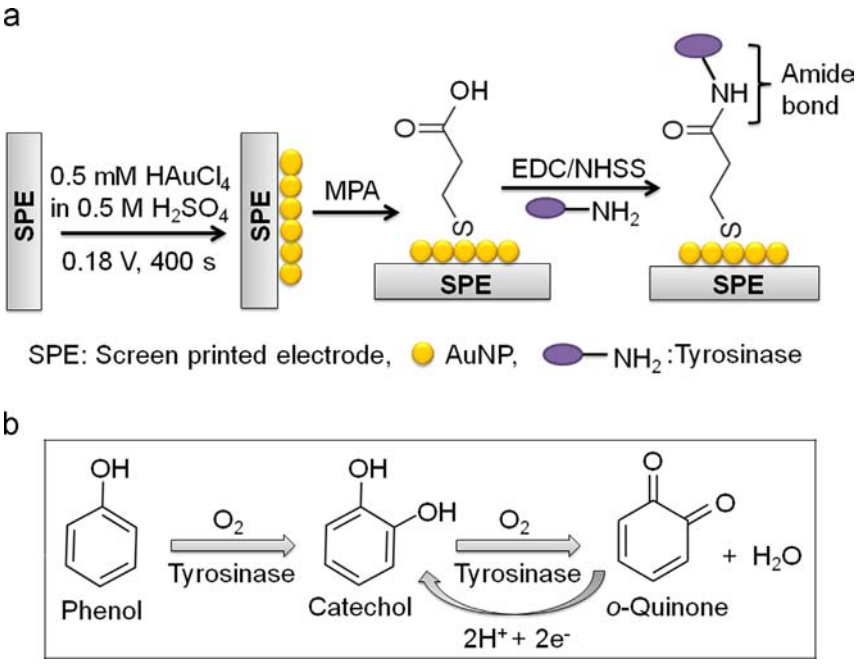

Scheme 1. (a) The fabrication procedure for tyrosinase modified AuNP's deposited on a screen printed carbon electrode (SPE) for phenol sensing. (b) The electrochemical detection of phenol via tyrosinase enzyme reaction. .

solution pH 6.5) was then dropped onto the EDC/NHSS activated Au surface and allowed to react at 4 °C for 15 h. This results in the covalent linking of random amine moieties from tyrosinase with the carboxylic terminal of the AuNP modified electrode. Prior to any electrochemical measurements, each biosensor was thoroughly washed with 0.1 M phosphate buffer solution (pH 7.0) and stored at 4 °C.

2.5. Electrochemical measurements

Electrochemical measurements for phenol sensing were carried out at room temperature using an electrochemical cell containing 5 mL of 0.1 M phosphate buffer solution (pH 7.0), followed by the successive addition of different volumes of concentrated phenol solution. For CV, a scan rate of 50 mV/s was used unless otherwise specified. For SWV measurements, a sweep potential between +0.05 V and −0.45 V with a step potential of 10 mV, an amplitude of 50 mV and a frequency of 15 Hz were used.

3. Results and discussion

3.1. Characterization of tyrosinase modified AuNPs on screen printed carbon electrodes for phenol detection

The electrodeposition of AuNPs onto a SPE was first verified by comparing cyclic voltammograms and scanning electron microscopy images of both the bare SPE and AuNPs on SPE. Fig. 1 compares cyclic voltammograms of bare and AuNP deposited SPEs in 0.5 M H_2SO_4 solution over a potential range from 0 to 1.50 V at a scan rate of 100 mVs^{-1}. For the bare SPE, no observable faradaic current appeared either on the forward or reverse scans within the potential window. Whereas, the cyclic voltammogram (solid line) for the AuNP modified SPE shows a typical of gold surface with the oxidative peak at 1.10 V (vs. Ag/AgCl) corresponding to gold oxide formation during the forward scan alongside the reduction peak at 0.50 V (vs. Ag/AgCl) responsible for the reduction of gold oxide during the reverse scan [22]. The presence of AuNPs deposited onto the SPE was further investigated using SEM. A typical rough surface was observed for bare SPE [30], while gold nanoparticles spread on the SPE surface was obtained for the AuNP modified SPE (Fig. 1b). The average diameter of these NPs is about 300 nm. In

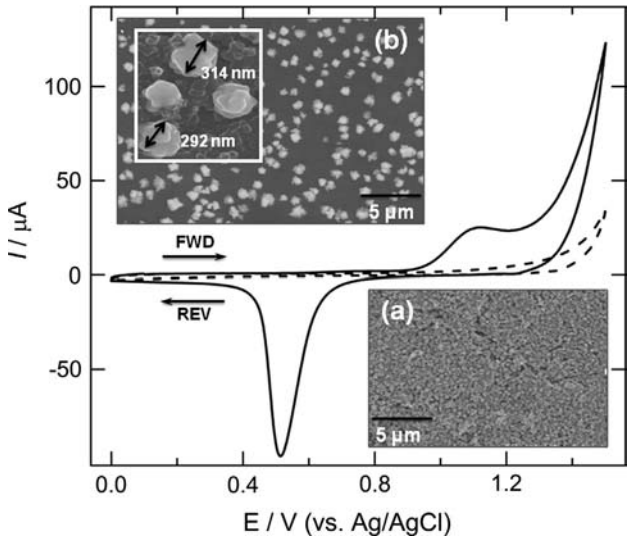

Fig. 1. Cyclic voltammograms of both bare (dotted line) and gold nanoparticle deposited SPE's (solid line). The supporting electrolyte was 0.5 M H_2SO_4, scan rate = 100 mV s^{-1}. Inset shows SEM images of the bare (a) and gold deposited SPE (b).

order to ensure the reproducibility of our Au deposition method, AuNPs were deposited onto 10 different screen printed electrodes using the same chronoamperometry parameter and 95% of the deposited chips showed the similar values of redox peak currents (solid line) as in Fig. 1. The reproducible gold deposition helps robust attachment of tyrosinase for reliable phenol sensing.

The tyrosinase modified Au nanoparticles on a screen printed electrode (Tyr–AuNP–SPE) biosensor via MPA and EDC/NHSS linking chemistry was first characterized for phenol sensing using cyclic voltammetry. Fig. 2a shows a series of cyclic voltammograms for different concentrations of phenol. A low background current was observed in the absence of phenol. As the phenol concentration increased, the current of the sigmoidal-shape response curves at −0.25 V (vs. Ag/AgCl) also increased. This is associated with the reduction of *ortho*-quinone liberated from the tyrosinase catalyzed reaction of phenol at the electrode surface (see also Scheme 1b). A linear relationship between the cathodic peak current and phenol concentration in the range between 0.94 ppm and 15 ppm is obtained with a slope of 0.42 µA ppm^{-1}. Five different phenol sensing chips were used for each concentration and the averaged values are presented in the Fig. 2a inset. In addition, scan rates were varied from 20 to 200 mVs^{-1} at a fixed concentration of phenol (Fig. S1a). The linear increment in the reduction peak as a function of the square root of the scan rate was observed indicative of a diffusion-controlled electrode process [31] (see Fig. S1b in the Supporting Information). The cyclic voltammetry experiments demonstrate that our portable biosensor can be used for the quantitative analysis of phenol in water samples and the tyrosinase immobilized on the AuNP modified SPE surface retains its bioactivity.

The analytical performance of the biosensor for phenol was further optimized by varying the pH of the buffer solution, system temperature and the concentration of enzyme used when immobilizing onto the AuNP modified electrode surface. These data are summarized in the Supporting Information (see Figs. S3–S5). The Tyr–AuNP–SPE biosensor was found to have an optimal performance for phenol detection under conditions of 0.1 M phosphate buffer solution at pH 7.0, 30 °C and 16.11 µg mL^{-1} of loading concentration of tyrosinase which is in good agreement with previous studies [32,33]. It should be noted that the improvement in performance on increasing the temperature above 25 °C was relatively small. Thus, considering also that this temperature is more feasible for field-based applications, the temperature at 25 °C was chosen throughout the remainder of this study.

3.2. Determination of phenol using square wave voltammetry

Since square wave voltammetry (SWV) has been widely used to improve the sensitivity of an amperometric sensor by measuring a net current which is larger than either the forward or reverse components alongside fast scan rates enabling a reduction of the analysis time [34], we employed SWV to enhance the sensitivity of our sensors for phenol detection. Fig. 2b shows the square wave voltammograms of the Tyr–AuNP–SPE for the different concentrations of phenol ranging from 47 ppb–15 ppm. In the absence of phenol, no peak response was observed at the potential range from +0.05 V to −0.45 V (Fig. 2b, i). Whereas, a sharp and well-defined peak at about −0.28 V assigned to the reduction of *o*-quinone species was observed to increase with respect to the increase in the phenol concentration (Fig. 2b ii–vi). A fast response time of about 3 s for a single phenol concentration measurement was also obtained.

Concentration dependence of the SWV response was analyzed by plotting the peak current over a range of both low and high phenol concentrations which reveal two different linearly

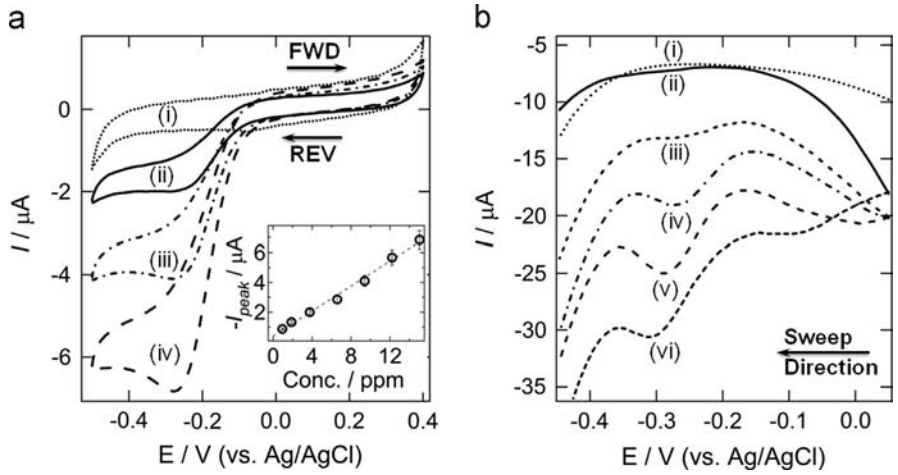

Fig. 2. Representative (a) cyclic and (b) square wave voltammograms for the sensing of different concentrations of phenol using tyrosinase modified AuNP screen printed electrodes. In (a), a scan rate of 50 mVs^{-1} was used. (i) In the absence of phenol and in the presence of (ii) 3.76, (iii) 9.4 and (iv) 15 ppm phenol. Inset graph in (a) shows a plot of the reduction peak current of *o*-quinone species released from the reaction of tyrosinase and phenol as a function of the phenol concentration. In (b), (i) in the absence of phenol, and in the presence of (ii) 0.047, (iii) 0.4, (iv) 0.8, (v) 5.0 and (vi) 15 ppm phenol. A step potential of 10 mV, an amplitude of 50 mV and a frequency of 15 Hz were used. 0.1 M phosphate buffer solution (pH 7.0) were used for both (a) and (b).

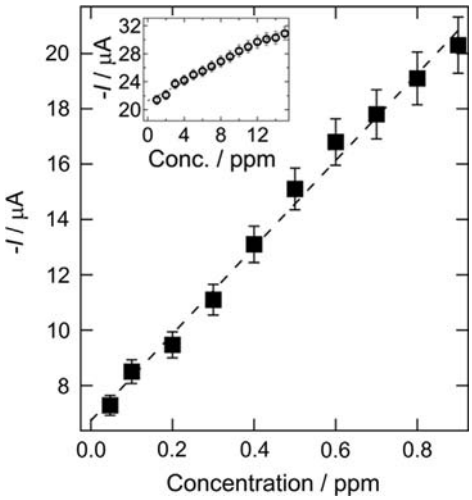

Fig. 3. Plots of SWV peak current vs. various concentrations of phenol from 47 ppb to 900 ppb. Inset shows a plot of peak current as a function of an extended concentration range from 1 to 15 ppm. All SWV experimental conditions are the same as in Fig. 2(b). Some of the data points are taken from Fig. 2(a).

dependent segments (see Fig. 3). Each data point represents the average of five separate measurements with five different chips for a
single phenol concentration. For the low concentration region (47 ppb–900 ppb), a slope of 15.67 μA ppm^{-1} was obtained, which is more sensitive than that of 0.68 μA ppm^{-1} obtained for the higher concentration range between 1.0 ppm to 15 ppm (Fig. 3 inset). A detectable concentration of 47 ppb phenol ($S/N=3$) was achieved, which is comparable to previously reported tyrosinase modified electrochemical biosensors including tyroinase–ZnO nanorods modified gold electrode [35] and a tyrosinase–ferrocene modified screen printed electrode [36]. In addition, the long-term stability of the sensor was also tested by repeatedly measuring the response of a prepared sensor at a fixed phenol concentration of 2 ppm eight times per every day while the sensor was kept in the 0.1 M phosphate buffer (pH 7.0) all the time. A relative standard deviation (RSD) value of 11.1% was obtained and the sensor could be used for 3 days. However, about 14% of the initial current response was diminished after 4 days (see Fig. S6).

Chip-to-chip variation was also assessed under optimal SWV measurement conditions with the data shown in the Supporting Information (Fig. S7) comparing repeat measurements for different electrodes at a fixed phenol concentration of 1 ppm. The total current response obtained was found to be reasonably reproducible with a RSD value of 12.3% (Fig. S7). This can be attributed to possible difficulties in conserving the same enzyme activity along with the surface density of AuNP's on the carbon electrode for each preparation. However, all electrodes showed linearity over the detectable phenol concentration range. Further investigation is required to improve the reproducibility of the biosensor.

Prior to performing an environmental water sample analysis, potential sample matrix effects on the electrochemical phenol sensor such as electrolyte condition and interference species were further investigated. For example, a river water sample may not contain sufficient supporting electrolyte or have a non-neutral pH, both parameters are important for the tyrosinase reaction and electrochemical performance. The developed biosensor was tested by detecting different concentrations of a phenol standard solution (Accustandard) dissolved in both tap water and buffered solution. Comparison of SWV responses with respect to the phenol concentration prepared in both 0.1 M phosphate buffer solution (pH 7.0) and tap water (pH 7.0) are shown in Fig. 4. Each data point per each phenol concentration is obtained by averaging five separate measurements with five different chips. It is interesting to note that a significant change in the peak current response vs. the phenol concentration is achieved depending upon the water matrix; in the presence of phosphate buffer, a linear fit with a slope of 0.012 μA ppb^{-1} was obtained for the concentration range from 75 ppb to 900 ppb (Fig. 4a), while a slope of 0.0067 μA ppb^{-1} was obtained for tap water. For the case of a higher concentration range from 1.0 ppm up to 10 ppm (Fig. 4b), a linear fit with slopes of 3.34 μA ppm^{-1} and 1.01 μA ppm^{-1} was obtained for the buffer solution and tap water, respectively. Overall, the sensor response in the absence of any buffering condition was about 56% dampened than that of the phosphate buffer matrix, which is mainly due to the decrease in tyrosinase bioactivity.

The selectivity of the sensor for phenol in the presence of some common potential interfering species was also examined in phosphate buffer solution (pH 7.0) at a fixed concentration (940 ppb) of phenol. A 100 times excess of interfering agents including ascorbic acid, uric acid, divalent metal ionic species such as Pb^{2+}, Mg^{2+}, Zn^{2+}, Ca^{2+} and Cu^{2+} ions and anions such as

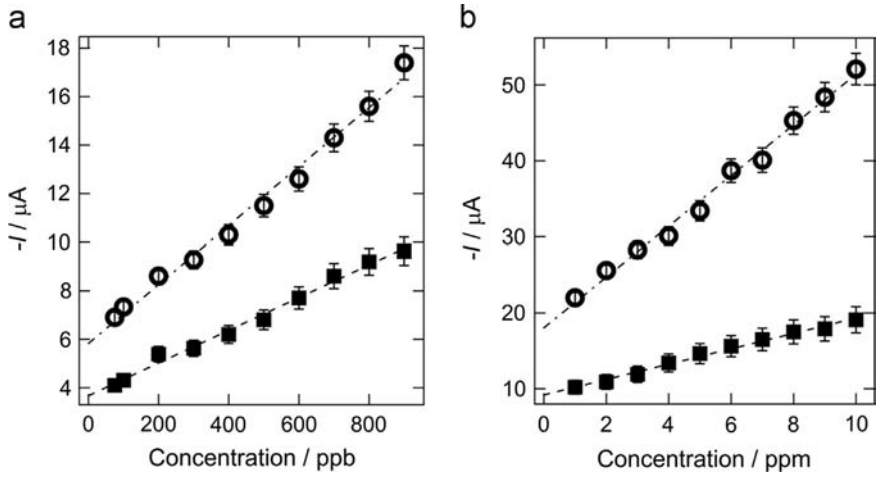

Fig. 4. Comparison of calibration plots for phenol detection using different water matrices. The circles and squares represent data from the analysis of phenol carried out in 0.1 M phosphate buffer (pH 7.0) solution and tap water, respectively. Dotted line represents a linear fit to the data. The phenol concentration was varied (a) from 75 ppb to 900 ppb and (b) from 1.0 ppm to 10 ppm.

Table 1
Comparison of river sample analyses using our sensor and autoanalyzer. Sample 1 is the sample from Sincheon river. Samples 2 and 3 are the Sincheon river water samples spiked with the phenol concentration of 75 and 200 ppb, respectively.

Sample number	Added phenol concentration (ppb)	Our sensor response[a], $-I_{peak}$ (μA)	Calibration plot in tap water, $-I_{peak}$ (μA)	Our method verification (ppb)	Autoanalyzer (ppb)
1	–	–	–	–	–
2	75	2.70	4.1	49.4	48
3	200	3.27	5.39	121.3	124.5

[a] Average responses of five measurements.

SO_4^{2-} and CO_3^{2-} ions were examined. Only Cu^{2+} ions with a selectivity coefficient of −2.25 showed a noticeable interference effect on our phenol sensing (see Table S1 in the Supporting Information).

3.3. *Environmental sample analysis; determination of phenol concentration in regional river water*

As a demonstration, our tyrosinase modified AuNP sensors and SWV were applied to the determination of phenol in a sample from the Sincheon river in S. Korea. Three different water samples were prepared; the first was the water sample itself and the other two samples were prepared by spiking different concentrations of phenol standard solutions (75 ppb and 200 ppb) to the Sincheon river samples. The SWV analysis results utilizing our sensor were compared to the data from a conventional autoanalyzer certified by the *Korea Environment & Water Works Institute*, which is one of the Korean-certified water quality evaluation centers. It can be concluded that Sincheon water contained almost no phenol or less than 50 ppb level of phenol which is our sensors detectability. This was also verified by the autoanalyzer results (see Table 1). As 75 and 200 ppb of the phenol standard solution were spiked into each of the Sincheon river water samples, the SWV peak current signature of the phenol increased with respect to the added phenol concentration. The peak currents for the samples spiked with 75 and 200 ppb of the standard phenol solution are −2.70 and −3.27 μA, respectively which reasonably correlates to the calibration plot obtained from the tap water matrix in Fig. 4a. A good agreement achieved in the results from both our sensing and the conventional autoanalyzer demonstrates that our method can be applied to real-time analysis of environmental water samples. However, there is scope for further improvements in the detectable range and sensitivity by developing a different surface attachment chemistry of tyrosinase to create a higher surface density of bioactive enzyme as well as optimization of the fractional surface coverage of gold nanostructures on the SPE. The Ministry of Land, Infrastructure and Transport in S. Korea has set the permittable limits of phenol at 5 ppb, 5 ppb and 10 ppb for drinking, agricultural and industrial water samples, respectively [37]. The gold standard for measurements at these levels remains gas chromatography/mass spectrometry and further efforts are required to introduce portable, selective biosensors capable of such measurements to the market.

4. Conclusion

An in-situ disposable biosensor consisted of tyrosinase tethered AuNPs on a screen printed carbon electrode is developed for the fast and sensitive detection of phenol in water samples. The use of electrodeposited gold nanoparticles resulted in an excellent sensitivity with a detectable phenol concnetration of 47 ppb. The sensor also shows a superb selectivity over various organic and inorganic interfering agents, which is one of the great advantages in addition to featuring fast analysis, cost effective and mass fabrication capabilities. In addition, the environmental field applicability of the sensor is demonstrated by the rapid analysis of regional river water with results that were in agreement with data validated using a conventional autoanalyzer. We envision that our disposable sensors can alternatively be applied to real-time monitoring of phenol contamination in environmental water samples, which can be of great interest in environmental science research and industries.

Acknowledgment

This research was supported by Basic Science Research Program through the National Research Foundation of Korea

(NRF) funded by the Ministry of Education, Science and Technology (2013R1A1A2A10005267).

Appendix A. Supplemantary material

Supplementary data associated with this article can be found in the online version at http://dx.doi.org/10.1016/j.talanta.2013.08.003.

References

[1] M. Llompart, M. Lourido, P. Landin, C. Garcia-Jares, R. Cela, J. Chromatogr. A 963 (2002) 137–148.
[2] F. Bosch, G. Font, J. Manes, Analyst 112 (1987) 1335–1337.
[3] X. Huang, N. Qiu, D. Yuan, J. Chromatogr. A 1194 (2008) 134–138.
[4] W. Wei, X.-B. Yin, X.-W. He, J. Chromatogr. A 1202 (2008) 212–215.
[5] J. Meng, C. Shi, B. Wei, W. Yu, C. Deng, X. Zhang, J. Chromatogr. A 1218 (2011) 2841–2847.
[6] G. Hanrahan, D.G. Patil, J. Wang, J. Environ. Monit. 6 (2004) 657–664.
[7] J. Abdullah, M. Ahmad, L.Y. Heng, N. Karuppiah, H. Sidek, Talanta 70 (2006) 527–532.
[8] Y.-C. Tsai, C.-C. Chiu, Sens. Actuators B 125 (2007) 10–16.
[9] J. Zhang, J. Lei, Y. Liu, J. Zhao, H. Ju, Biosens. Bioelectron. 24 (2009) 1858–1863.
[10] D. Shan, Q. Shi, D. Zhu, H. Xue, Talanta 72 (2007) 1767–1772.
[11] A. Chaubey, K.K. Pande, V.S. Singh, B.D. Malhotra, Anal. Chim. Acta 407 (2000) 97–103.
[12] J. Yu, S. Liu, H. Ju, Biosens. Bioelectron. 19 (2003) 509–514.
[13] H. Xue, Z. Shen, Talanta 57 (2002) 289–295.
[14] C. Vedrine, S. Fabiano, C. Tran-Minh, Talanta 59 (2003) 535–544.
[15] S. Hashemnia, S. Khayatzadeh, M. Hashemnia, J. Solid State Electrochem. 16 (2012) 473–479.
[16] Rajesh, W. Takashima K. Kaneto, Sensors Actuators B 102 (2004) 271–277.
[17] Y.L. Zhou, J.F. Zhi, Electrochem. Commun. 8 (2006) 1811–1816.
[18] G.-Y. Kim, J. Shim, M.-S. Kang, S.-H. Moon, J. Hazard. Mater. 156 (2008) 141–147.
[19] X. Luo, A. Morrin, A.J. Killard, M.R. Smyth, Electroanalysis 18 (2006) 319–326.
[20] S.A. Ansari, Q. Husain, Biotechnol. Adv. 30 (2012) 512–523.
[21] J.M. Pingarron, P. Yanez-Sedeno, A. Gonzalez-Cortes, Electrochim. Acta 53 (2008) 5848–5866.
[22] M.A. Alonso-Lomillo, C. Yardimci, O. Dominguez-Renedo, M.J. Arcos-Martinez, Anal. Chim. Acta 633 (2009) 51–56.
[23] J. Polte, T.T. Ahner, F. Delissen, S. Sokolov, F. Emmerling, A.F. Thunemann, R. Kraehnert, J. Am. Chem. Soc. 132 (2010) 1296–1301.
[24] C. Ziegler, A. Eychmuller, J. Phys. Chem. C 115 (2011) 4502–4506.
[25] H. Wender, M.L. Andreazza, R.R.B. Correia, S.R. Teixeira, J. Dupont, Nanoscale 3 (2011) 1240–1245.
[26] M. Fukushima, H. Yanagi, S. Hayashi, N. Suganuma, Y. Taniguchi, Thin Solid Films 438–439 (2003) 39–43.
[27] J. Wang, L. Wang, J. Di, Y. Tu, Talanta 77 (2009) 1454–1459.
[28] W.H. Binder, C. Kluger, M. Josipovic, C.J. Straif, G. Friedbacher, Macromolecules 39 (2006) 8092–8101.
[29] U.S. Mohanty, J. Appl. Electrochem. 41 (2011) 257–270.
[30] W. Song, D.-W. Li, Y.-T. Li, Y. Li, Y.-T. Long, Biosens. Bioelectron. 26 (2011) 3181–3186.
[31] Z. Dai, X. Xu, L. Wu, H. Ju, Electroanalysis 17 (2005) 1571–1577.
[32] Z. Liu, Y. Liu, H. Yang, Y. Yang, G. Shen, R. Yu, Anal. Chim. Acta 533 (2005) 3–9.
[33] J. Ren, T.-F. Kang, R. Xue, C.-N. Ge, S.-Y. Cheng, Microchim. Acta 174 (2011) 303–309.
[34] J. Wang, Analytical Electrochemistry, third ed., John Wiley & Sons, Inc., Hoboken, New Jersey (2006) 80–82.
[35] B.X. Gu, C.X. Xu, G.P. Zhu, S.Q. Liu, L.Y. Chen, X.S. Li, J. Phys. Chem. B 113 (2009) 377–381.
[36] M.R. Montereali, W. Vastarella, L.D. Seta, R. Pilloton, Int. J. Environ. Anal. Chem. 85 (2005) 795–806.
[37] ⟨http://www.wamis.go.kr/ (or www.wamis.go.kr/eng/overview.aspx)⟩.